ULTRAHIGH ENERGY NEUTRINO PHYSICS*

J. Kwiecinski[a], A.D. Martin[b] and A.M. Stasto[a]

[a] H. Niewodniczański Institute of Nuclear Physics
Radzikowskiego 152, Kraków, Poland
[b] Department of Physics, University of Durham
Durham, DH1 3LE, United Kingdom

(Received April 11, 2000)

We discuss a problem concerning the ultrahigh energy neutrino propagation through the Earth. We present calculation of the neutrino–nucleon cross section at high energies, based on the unified evolution equation at small x. We also show the solution of the transport equation for different neutrino fluxes originating from active galactic nuclei, gamma ray bursts and top-down model.

PACS numbers: 13.15.+g

1. Introduction

The ultrahigh energy neutrino physics is an interdisciplinary subject which can address many vital problems in astrophysics, particle physics and geophysics, for a review see [1, 2]. Neutrinos can traverse large distances without being disturbed and thus give us important information about distant astronomical objects like active galactic nuclei or gamma ray bursts. The ultrahigh energy neutrinos can have energies up to 10^{12} GeV, much larger than currently accessible at present colliders, like HERA. At these ultrahigh energies the structure of nucleon is probed at very small values of Bjorken x. It means that we are possibly entering a region in which partons have large density. Therefore detailed knowledge of parton distribution function at very small x is vital to estimate the neutrino–nucleon cross section. This cross section rises strongly with energy and therefore neutrino propagation through the Earth can be affected by the increased interaction with matter at these ultrahigh energies. Thus it is necessary to consider the effect of attenuation of high energy neutrinos while traversing the Earth. This

* Presented at the Cracow Epiphany Conference on Neutrinos in Physics and Astrophysics, Cracow, Poland, January 6–9, 2000.

phenomenon could be used as a possible method of the "Earth tomography" by neutrinos. All these topics will be studied at large neutrino telescopes like AMANDA, NESTOR and ANTARES (for review see [3]).

In this paper we present a method of calculation the neutrino–nucleon cross section using gluon and quark distributions obtained from a unified evolution equation for small x [4]. This equation embodies both DGLAP and BFKL evolutions on equal footing as well as important subleading effects via consistency constraint [5]. This constraint limits the virtualities of the exchanged gluon momenta in the ladder to their transverse components. We then extrapolate the results to ultrahigh energies and compare the predictions with the other, based on standard global parton analysis [1, 6].

We use the resulting cross section as an input to the transport equation [7] for the neutrino flux penetrating the Earth. We solve this equation for different incident angles as well as different input neutrino fluxes originating from active galactic nuclei, gamma ray bursts and a sample top-down model.

The details of the calculation has been presented elsewhere [8].

2. Sources of ultrahigh energy neutrinos

Neutrinos have the advantage that they are weakly interacting with matter and they are hardly absorbed when travelling along large distances. On the other hand cosmic rays are being absorbed through the following interactions:

- pair production: $\gamma_{\rm CR} + \gamma_{\rm BR} \to e^+e^-$
- inverse Compton scattering: $e_{\rm CR} + \gamma_{\rm BR} \to e + \gamma$
- photoproduction of pion: $p_{\rm CR} + \gamma_{\rm BR} \to p + N\pi$
- nuclei fragmentation by photo-pion interactions

These reactions cause that the spectrum of the cosmic rays has the GZK cutoff [9] around 10^{19}eV. Therefore neutrinos are the best candidates for supplying information about distant objects. The possible sources of highly energetic neutrinos are:

- active galactic nuclei
- gamma ray bursts
- top-down models

Active galactic nuclei are the most powerful sources of radiation in the whole Universe. The engine of the AGN is the supermassive black hole with mass billion times larger than the mass of the sun. Surrounding the black hole is the accretion disc usually accompanied by two jets. The spectrum of the emitted photons spreads from radio waves to TeV energies. The jets are the sources of the most energetic gamma rays, since the particles (electrons and possibly protons) are accelerated in blobs along the jets with Lorenz factor $\gamma \sim 10$. Electrons loose energy via synchrotron radiation thus producing very energetic photons. If protons are also accelerated then they can interact with the ambient photons producing pions. Consequently strong flux of neutrinos will be produced [10–12].

Gamma ray bursts are also very probable sources of neutrinos. Although the underlying event of GRB's is not entirely known the present knowledge is consistent that the bursts are produced as a relativistically expanding fireball which initial radius was around 100 km. The original state which is opaque to light expands in a relativistic shock with $\gamma \sim 300$ to the point where it becomes optically thin and produces intensive gamma ray spectrum. As in the case of AGN, the acceleration of protons can result in the production of neutrinos because they will photoproduce pions and in the end neutrinos will emerge [13].

Top-down models are the most speculative scenarios of producing neutrino fluxes at ultrahigh energies. In these models one assumes that the particles are not accelerated but are rather produced as a result of the decay of the supermassive particles $M_x \sim 10^{14}$–10^{16} GeV. These particles could emerge as a decay of some topological defects: superconducting strings or magnetic monopoles. The top-down models produce quite hard spectrum of neutrinos extending beyond 10^{12} GeV and they were proposed as a possible solution to the GZK cutoff [14].

3. Neutrino–nucleon cross section

The dominant interaction for neutrinos is the neutrino–nucleon interaction. It has the largest value of the cross section, and is dominating over the interaction with electrons. There is however one exception: resonant W production in $\bar{\nu_e}\, e^-$ interaction at $E_\nu = 6.4 \times 10^5$ GeV. At this energy this process dominates by 2 orders of magnitude over other contributions.

The neutrino–nucleon interaction can be visualised in Fig. 1. Here l is the incoming neutrino of four momentum k and l' is the outgoing neutrino or charged lepton with four momentum k'. N is the target nucleon with four momentum p and X is the arbitrary hadronic final state. This deep inelastic scattering process can be described using two standard variables: $q^2 = -Q^2 < 0$ is the four momentum squared of the exchanged vector boson,

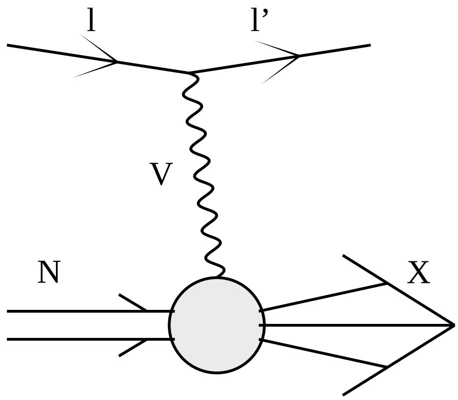

Fig. 1. Deep inelastic scattering

and $x = \frac{Q^2}{2p\cdot q}$ is the standard Bjorken scaling variable. At high energies (up to 10^{12} GeV), very small values of x can be probed because

$$x \sim \frac{M_V^2}{2M_N \nu} \sim 10^{-8}\,, \tag{1}$$

where M_V is the mass of the heavy vector boson, M_N is the nucleon mass and ν is the energy of the exchanged vector boson. These are values of x which are not accessible at present electron–proton colliders (for example HERA goes down to 10^{-5} at fairly low Q^2). Therefore, a detailed knowledge of parton distributions at these small values of x are required. We propose to use the unified BFKL/DGLAP evolution equation [4]. We shall start at first with the pure leading order BFKL equation [15] for the unintegrated gluon distribution function $f(x,k^2)$ in the following form:

$$\begin{aligned} f(x,k^2) \;&=\; f^{(0)}(x,k^2) + \bar{\alpha}_{\rm s} k^2 \int\limits_x^1 \frac{dz}{z} \int \frac{dk'^2}{k'^2} \left\{ \frac{f\left(\frac{x}{z},k'^2\right) - f\left(\frac{x}{z},k^2\right)}{|k'^2-k^2|} \right. \\ &\left. + \frac{f\left(\frac{x}{z},k^2\right)}{[4k'^4+k^4]^{\frac{1}{2}}} \right\}, \end{aligned} \tag{2}$$

where $\bar{\alpha}_{\rm s} = N_c \alpha_{\rm s}/\pi$ and $k = k_{\rm T}, k' = k'_{\rm T}$ denote the transverse momenta of the gluons, see Fig. 2. The term in the integrand containing $f(x/z,k'^2)$ corresponds to real gluon emission, whereas the terms involving $f(x/z,k^2)$ represent the virtual contributions and lead to the Reggeization of the t-channel exchanged gluons. The inhomogeneous driving term $f^{(0)}$ is the input function and will be specified later. This is the leading order in

$\ln(1/x)$ equation which gives the very well known intercept for the gluon $\lambda = \bar{\alpha_s} 4 \ln 2$. The next to leading contribution to the t-channel exchange at high energies has been already calculated [16]. It yields however very large correction to the intercept making it physically unreliable. It occurred, that the resummation of the subleading effects should be performed in order to get physically reliable results [17, 18]. Different forms of resummation has been already proposed in the literature. It appears that the imposition of the consistency constraint [5] which limits the phase-space available for the real emission term provides with the partial resummation of the subleading effects. This constraint arises from the fact that in the high energy limit the virtualities of the exchanged momenta are dominated by their transverse parts. By imposition of this constraint one obtains nice physical picture in which the subleading effects are resummed by the limitation of the phase space. The result for the gluon intercept yields reasonable value which is stable, *i.e.* does not become negative. Second improvement to the equation (2) is the inclusion of the DGLAP terms which are important for large values of x and the overall normalisation of the resulting gluon distribution function. We do also include the quark driving term in Eq. (2). The resulting evolution equation for the gluon has the following form:

$$
\begin{aligned}
&f(x,k^2) = \tilde{f}^{(0)}(x,k^2) \\
&+\bar{\alpha}_{\rm s}(k^2)k^2 \int\limits_x^1 \frac{dz}{z} \int\limits_{k_0^2} \frac{dk'^2}{k'^2} \left\{ \frac{f\left(\frac{x}{z},k'^2\right)\Theta\left(\frac{k^2}{z}-k'^2\right) - f\left(\frac{x}{z},k^2\right)}{|k'^2-k^2|} + \frac{f\left(\frac{x}{z},k^2\right)}{[4k'^4+k^4]^{\frac{1}{2}}} \right\} \\
&+\bar{\alpha}_{\rm s}(k^2) \int\limits_x^1 \frac{dz}{z}\left(\frac{z}{6}P_{gg}(z)-1\right) \int\limits_{k_0^2}^{k^2} \frac{dk'^2}{k'^2} f\left(\frac{x}{z},k'^2\right) + \frac{\alpha_{\rm s}(k^2)}{2\pi} \int\limits_x^1 dz P_{gq}(z) \Sigma\left(\frac{x}{z},k^2\right).
\end{aligned}
\tag{3}
$$

We specify the driving term in the following form:

$$
\tilde{f}^{(0)}(x,k^2) = \frac{\alpha_{\rm s}(k^2)}{2\pi} \int\limits_x^1 dz P_{gg}(z) \frac{x}{z} g\left(\frac{x}{z},k_0^2\right) . \tag{4}
$$

Let us note that the inhomogeneous term has been entirely specified in terms of the standard integrated gluon distribution function at the infrared cutoff k_0^2 and that the BFKL/DGLAP evolution only takes place above this cutoff. The last term in Eq. (3) is the contribution of the quark distribution to the gluon evolution

$$
\Sigma = \sum_q x(q+\bar{q}) = \sum_q (S_q + V_q) , \tag{5}
$$

where S and V denote the sea and valence quark momentum distributions. The gluon, in turn, helps to drive the sea quark distribution through the $g \to q\bar{q}$ transition. Thus equation (3) has to be solved simultaneously with an equivalent equation for $\Sigma(x,k^2)$. We use the $k_{\rm T}$ factorisation formula [19], see Fig. 2 as a basis for our evolution equation for the quark distribution.

$$S_q(x,Q^2) = \int_x^1 \frac{dz}{z} \int \frac{dk^2}{k^2} S^q_{\rm box}(z,k^2,Q^2) f\left(\frac{x}{z},k^2\right) , \tag{6}$$

where $S^{\rm box}$ describes the quark box (and crossed-box) contribution shown in Fig. 2 and can be interpreted as a partonic structure function. It has been

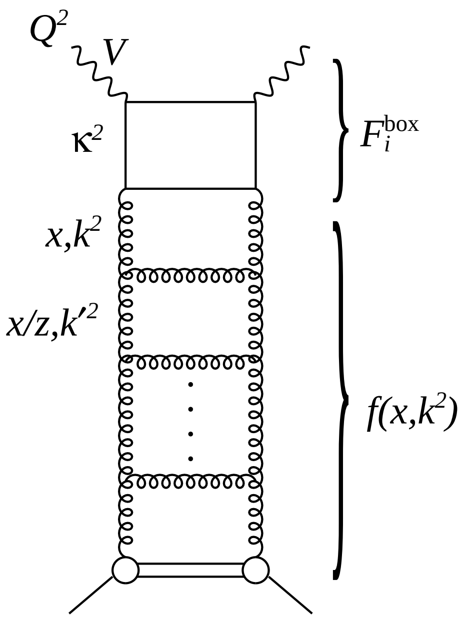

Fig. 2. Diagrammatic representation of the $k_{\rm T}$-factorization formula. At lowest order in $\alpha_{\rm s}$ the gauge boson–gluon fusion processes, $Vg \to q\bar{q}$, are given by the quark box shown (together with the crossed box). The variables κ, k and k' denote the transverse momenta of the indicated virtual particles.

shown (see for example [20, 4]) that the $\ln(1/x)$ effects are also resummed and play important role in the $k_{\rm T}$ factorisation prescription. In order to get the complete set of evolution equations we also have to add quark–quark splittings (which are small numerically anyway) and the valence quarks, which we take from the set of parametrisations. Thus our complete equation for the singlet quark distribution reads as follows:

$$\begin{aligned}\Sigma(x,k^2) &= S_{\text{non}-p}(x) + \sum_q \int_x^a \frac{dz}{z} S_q^{\text{box}}(z,k'^2=0,k^2)\frac{x}{z} g\left(\frac{x}{z},k_0^2\right) \\ &+ \sum_q \int_{k_0^2}^{\infty} \frac{dk'^2}{k'^2} \int_x^1 \frac{dz}{z} S_q^{\text{box}}(z,k'^2,k^2) f\left(\frac{x}{z},k'^2\right) + V(x,k^2) \\ &+ \int_{k_0^2}^{k^2} \frac{dk'^2}{k'^2}\frac{\alpha_{\text{s}}(k'^2)}{2\pi} \int_x^1 dz P_{qq}(z) S_{uds}\left(\frac{x}{z},k'^2\right) , \end{aligned} \tag{7}$$

where $a = (1+4m_q^2/Q^2)^{-1}$ and $V = x(u_v + d_v)$. Equations (3) and (7) form a set of coupled integral equations for the unknown functions $f(x,k^2)$ and $\Sigma(x,k^2)$. We solve them assuming simple parametric form of the inputs:

$$\begin{aligned} xg(x,k_0^2) &= N(1-x)^{\beta} , \\ S_{\text{non}-p}(x) &= C_p(1-x)^8 x^{-0.08} . \end{aligned} \tag{8}$$

We have used this set of coupled equations to calculate F_2 structure function at HERA, and we have therefore fixed the values of the free parameters N, β and C_p. We then used the resulting parton distribution functions in order to calculate the neutrino–nucleon cross section at high energies. We calculate the cross sections from the usual formula:

$$\begin{aligned}\frac{d^2\sigma^{\nu,\overline{\nu}}}{dxdy} &= \frac{G_{\text{F}}ME}{\pi}\left(\frac{M_i^2}{Q^2+M_i^2}\right)^2 \left\{\frac{1+(1-y)^2}{2} F_2^{\nu}(x,Q^2)\right. \\ &\left. - \frac{y^2}{2} F_L^{\nu}(x,Q^2) \pm y\left(1-\frac{y}{2}\right) xF_3^{\nu}(x,Q^2)\right\} , \end{aligned} \tag{9}$$

where G_{F} is the Fermi coupling constant, M is the proton mass, E is the laboratory energy of the neutrino and $y = Q^2/xs$. The mass M_i is either M_W or M_Z according to whether we are calculating charged current (CC) or neutral current (NC) neutrino interactions.

Functions F_2^{ν}, F_L^{ν} and xF_3^{ν} are of course usual structure functions which can be calculated from the parton distribution functions. In Fig. 3 we show the plot of $\sigma(\nu N)$ as a function of energy of the neutrino E_{ν}. One observes strong rise, nearly 8 decades with increasing energy from 10 to 10^{12} GeV. The shape of the curves up to 10^5 GeV is determined by the valence quarks whereas beyond 10^6 GeV everything is driven by the sea quarks. One also notes that the charged current contribution is dominating over the neutral current by factor 3.

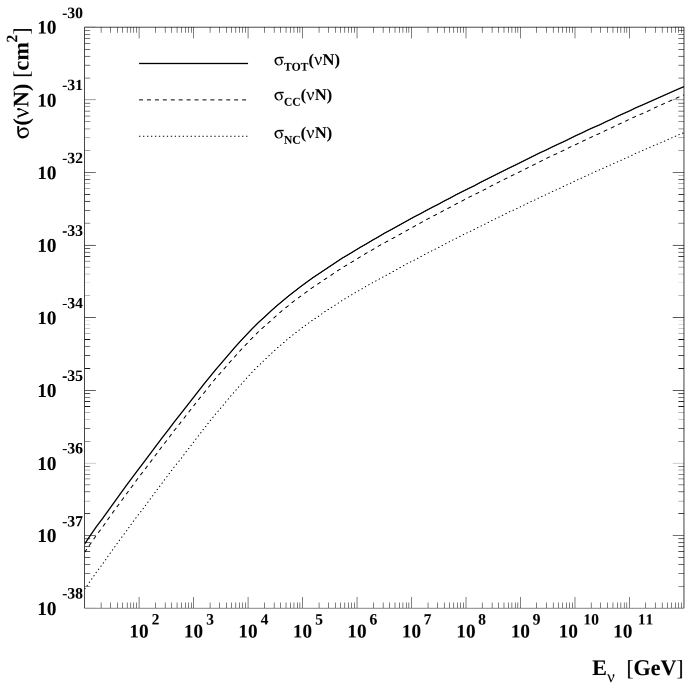

Fig. 3. The total νN cross section and its decomposition into charged and neutral current contributions as a function of the laboratory neutrino energy.

4. Transport equation

Neutrinos at ultrahigh energies can be quite strongly attenuated when traversing the Earth. Apart from standard absorption neutrinos can undergo regeneration due to neutral current interactions. Charged current interactions remove neutrinos from the flux, but neutral current interaction cause neutrinos to reappear at lower energies. These both effects can be calculated using the transport equation for the neutrino flux $I(E,\tau)$ proposed in [7]:

$$\frac{dI(E,\tau)}{d\tau} = -\sigma_{\rm TOT}(E)I(E,\tau) + \int \frac{dy}{1-y}\frac{d\sigma_{\rm NC}(E',y)}{dy}I(E',\tau)\,, \qquad (10)$$

where $\sigma_{\rm TOT} = \sigma_{\rm CC} + \sigma_{\rm NC}$ and where y is, as usual, the fractional energy loss such that

$$E' = \frac{E}{1-y}\,. \qquad (11)$$

The variable τ is the number density of nucleons n integrated along a path of length z through the Earth

$$\tau(z) \ = \int\limits_0^z dz' \, n(z') . \tag{12}$$

The number density $n(z)$ is defined as $n(z) = N_{\mathrm{A}}\, \rho(z)$ where $\rho(z)$ is the density of Earth along the neutrino path length z and N_{A} is the Avogadro number. The number of nucleons τ encountered along the path z depends upon the nadir angle θ between the normal to the Earth's surface (passing through the detector) and the direction of the neutrino beam incident on the detector.

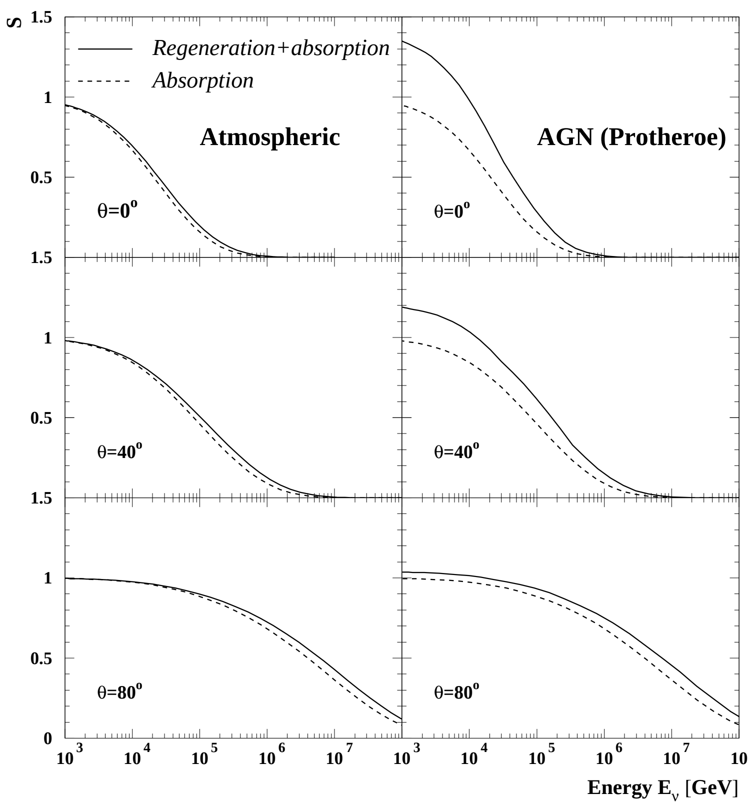

Fig. 4. The shadowing factor S of (13) for two different initial neutrino fluxes incident at three different nadir angles on a detector. The angle $\theta = 0°$ corresponds to penetration right through the Earth's diameter. The two curves on each plot show the shadowing factor with and without NC regeneration included.

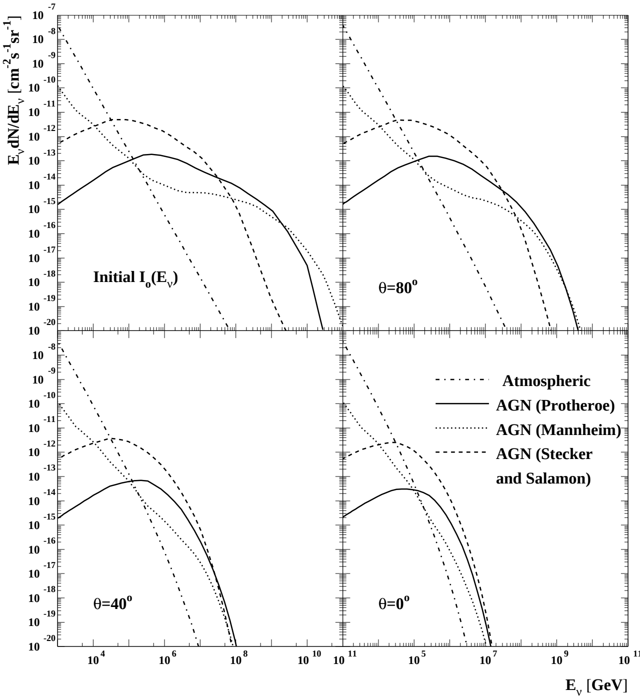

Fig. 5. The initial flux $I_0(E)$ and the flux at the detector $I(E)$ for three different nadir angles corresponding to three models for AGN neutrinos [10–12]. The background atmospheric neutrino flux is also shown. All the fluxes are given for muon neutrinos. The corresponding fluxes from [10–12] were given originally for muon neutrinos and anti-neutrinos, and their value has been divided by factor 2.

In order to calculate the change of the intensity of the flux with the incident angle one needs to know the density profile of the Earth. We have used the model by Dziewoński [21]. Using this parametrisation of the Earth density and the cross sections calculated from the unified BFKL/DGLAP equation. In Fig. 4 we show the shadowing factor,

$$S(E,\tau) \;=\; \frac{I(E,\tau)}{I^0(E)}\,, \tag{13}$$

where $I^0(E) = I(E,\tau)$ is the initial flux at the surface of the Earth. We present S as a function of the energy and for different incident angles. The curves exhibit strong suppression for large paths in matter and the energies above 10^6 GeV. Also, the curves corresponding to the flux from AGN [10], show that the regeneration is important for flat fluxes and large paths. The same effect is nearly negligible in the case of steeply falling atmospheric spectrum [22].

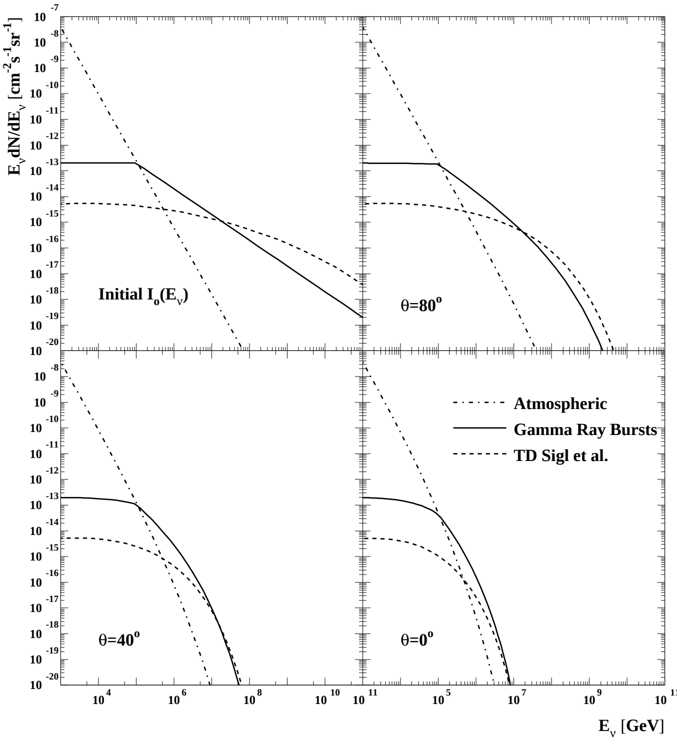

Fig. 6. The initial flux $I_0(E)$ and the flux at the detector $I(E)$ for three different nadir angles corresponding to the model of gamma ray burst [13] and the top-down model [14]. The background atmospheric neutrino flux is also shown. All the fluxes are given for muon neutrinos.

In Figs. 5 and 6 we show complete simulation for different incident fluxes corresponding to the active galactic nuclei [10–12], gamma ray bursts [13] and a sample top-down model [14]. Similar effects of strong attenuation are observed for large energies $\sim 10^6$ GeV and large paths. This suggests that one will have to choose suitable angle of the observation in order to avoid large muon background from the atmosphere and yet be able to detect the highly energetic neutrinos which are likely to be absorbed by the matter in Earth.

5. Summary

In this paper we have examined the interactions of ultrahigh energy neutrinos with matter. As the cross section rises with increasing energy the absorption by matter becomes interestingly large. We have seen that the Earth becomes essentially opaque to ultrahigh energy neutrinos. We have calculated neutrino–nucleon cross section using the unified DGLAP/BFKL evolution equations which treat leading $\ln(Q^2)$ and $\ln(1/x)$ on equal footing. These equations also resum important subleading effects in $\ln(1/x)$ via imposition of consistency constraint. We believe that this form of the evolution is most appropriate in the regime where the parton density is large. The results for the cross section has been compared with the other based on the standard global parton analysis. In that way the uncertainty due to parton density extrapolation has been diminished to 40%. We have then used the resulting cross sections and solved the transport equation for the neutrinos travelling through the Earth. We have found that the attenuation is large for high energies, above 10^6 GeV and long paths in matter. We have also found that the regeneration due to neutral current interactions becomes important for flat spectra (like these originating from active galactic nuclei) and large paths. We have simulated the penetration through the Earth for different neutrino fluxes: active galactic nuclei, gamma ray bursts and top-down models. The large attenuation effect reduces substantially the flux for small nadir angles. There is however a window for observation of AGN fluxes by the km^3 detectors.

This research has been supported in part by the Polish State Committee for Scientific Research (KBN) grant N0 2 P03B 89 13 and by the EU Fourth Framework Programme "Training and Mobility of Researchers", Network "Quantum Chromodynamics and the Deep Structure of Elementary Particles", contract FMRX–CT98–0194.

REFERENCES

[1] R. Gandhi, C. Quigg, M. Reno, I. Sarcevic, *Astropart. Phys.* **5**, 81 (1996).

[2] R. Gandhi, C. Quigg, M. Reno, I. Sarcevic, *Phys. Rev.* **D58**, 093009 (1998).

[3] F. Halzen, MADPH-98-1088, `astro-ph/9810368`.

[4] J. Kwiecinski, A.D. Martin, A.M. Stasto, *Phys. Rev.* **D56**, 3991 (1997); J. Kwiecinski, A.D. Martin, A.M. Stasto, *Acta Phys. Pol.* **B28**, 2577 (1997).

[5] B. Andersson, G. Gustafson, J. Samuelsson, Lund preprint, LU-TP 95-13; B. Andersson, G. Gustafson, H. Kharraziha, J. Samuelsson, *Z. Phys.* **C71**, 613 (1996).

[6] M. Glück, S. Kretzer, E. Reya, *Astropart. Phys.* **11**, 327 (1999).

[7] A. Nicolaidis, A. Taramopoulos, *Phys.Lett.* **B386**, 211 (1996).

[8] J. Kwiecinski, A.D. Martin, A.M. Stasto, *Phys. Rev.* **D59**, 093002 (1999).

[9] K. Greisen, *Phys. Rev. Lett.* **16**, 748 (1966); G.T. Zatsepin, V.A. Kuzmin, *JETP Lett.* **4**, 78 (1966).

[10] R.J. Protheroe, *Accretion Phenomena and Related Outflows,* IAU Colloq. 163, ed. D. Wickramashinghe *et al.*, 1996, `astro-ph/9607165`; Talk at Neutrino 98, Takayama 4-9 June 1998, `astro-ph/9809144`; ADP-AT-96-15, *Towards the Millennium in Astrophysics: Problems and Prospects*, Erice 1996, eds. M.M. Shapiro and J.P. Wefel, World Scientific, Singapore `astro-ph/9612213`.

[11] K. Mannheim, *Astropart. Phys.* **3**, 295 (1995).

[12] F.W. Stecker, H. Salamon, "TeV Gamma-Ray Astrophysics", 1994, p. 341. `astro-ph/9501064`.

[13] E. Waxman, J. Bahcall, *Phys. Rev. Lett.* **78**, 2292 (1997).

[14] G. Sigl, S. Lee, P. Bhattacharjee, S. Yoshida, *Phys. Rev.* **D59**, 043504 (1999); G. Sigl, S. Lee, D. N. Schramm, P. Coppi, *Phys. Lett.* **B392**, 129 (1997).

[15] E.A. Kuraev, L.N. Lipatov, V.S. Fadin, *Zh. Eksp. Teor. Fiz.* **72**, 373 (1977), (*Sov. Phys. JETP* **45**, 199 (1977); Ya. Balitzkij, L.N. Lipatov, *Yad. Fiz.* **28**, 1597 (1978), (*Sov. J. Nucl. Phys.* **28**, 822 (1978)), J.B. Bronzan, R.L. Sugar, *Phys. Rev.* **D17**, 585 (1978); T. Jaroszewicz, *Acta. Phys. Pol.* **B11**, 965 (1980).

[16] see for example: L.N. Lipatov, V.S. Fadin, *Sov. J. Nucl. Phys.* **50**, 712 (1989); V.S. Fadin, L.N. Lipatov, *Nucl. Phys.* **B406**, 259 (1993); *Nucl. Phys.* **B477**, 767 (1996); M. Ciafaloni, *Phys. Lett.* **B429**, 363 (1998); G. Camici, M. Ciafaloni, *Nucl. Phys.* **B496**, 305 (1997);

[17] G.P. Salam, *J. High Energy Phys.* **07**, 019 (1998).

[18] M. Ciafaloni, D. Colferai, G.P. Salam, *Phys. Rev.* **D60**, 114036 (1999); M. Ciafaloni, D. Colferai, G.P. Salam, *J. High Energy Phys.* **10**, 017 (1999).

[19] S. Catani, M. Ciafaloni, F. Hautmann, *Phys. Lett.* **B242**, 97 (1990); *Nucl. Phys.* **366**, 657 (1991); J.C. Collins, R.K. Ellis, *Nucl. Phys.* **B360**, 3 (1991); S. Catani, F. Hautmann, *Nucl. Phys.* **B427**, 475 (1994); M. Ciafaloni, *Phys. Lett.* **B356**, 74 (1995).

[20] R. Thorne, *Nucl. Phys.* **B512**, 323 (1998).

[21] A.M. Dziewonski, D.L. Anderson, Preliminary Reference Earth Model, *Phys. Earth Planet. Inter.* **25**, 297 (1981).

[22] L.V. Volkova, *Yad. Fiz.* **31**, 1510 (1980), (*Sov. J. Nucl. Phys.* **31**, 784 (1980)).